First dataset of ^{236}U and ^{233}U around the Greenland coast: A 5-year snapshot (2012–2016)

Qiao, Jixin; Hain, Karin; Steier, Peter

Published in:
Chemosphere

Link to article, DOI:
10.1016/j.chemosphere.2020.127185

Publication date:
2020

Document Version
Peer reviewed version

First dataset of ^{236}U and ^{233}U around the Greenland coast: A 5-year snapshot (2012–2016)

Jixin Qiao, Karin Hain, Peter Steier

PII: S0045-6535(20)31378-3

DOI: https://doi.org/10.1016/j.chemosphere.2020.127185

Reference: CHEM 127185

To appear in: *ECSN*

Received Date: 6 March 2020

Revised Date: 18 May 2020

Accepted Date: 21 May 2020

Please cite this article as: Qiao, J., Hain, K., Steier, P., First dataset of ^{236}U and ^{233}U around the Greenland coast: A 5-year snapshot (2012–2016), *Chemosphere* (2020), doi: https://doi.org/10.1016/j.chemosphere.2020.127185.

Graphic Abstract

First dataset of ^{236}U and ^{233}U around the Greenland coast: a 5-year snapshot (2012-2016)

Jixin Qiao,[a1] *Karin Hain* [b], *Peter Steier* [b]

[a] Department of Environmental Engineering, Technical University of Denmark, DK-4000 Roskilde, Denmark

[b] VERA Laboratory, Faculty of Physics – Isotope Physics, University of Vienna, Währinger Straße 17, A-1090 Vienna, Austria

[1] Corresponding author. Tel: +45 46775367. E-mail: jiqi@dtu.dk

ABSTRACT

We report the first combined dataset of ^{236}U and ^{233}U in the Greenland marine environment during the period of 2012-2016. Results are discussed in terms of time evolution and spatial distribution of ^{236}U concentration, and atomic ratios of $^{236}U/^{238}U$ and $^{233}U/^{236}U$. ^{236}U concentrations along the Greenland coast are distributed within a relatively narrow range of (0.7-12.9) × 10^{7} atom/L, corresponding to $^{236}U/^{238}U$ atomic ratios of (1.1-15.5) × 10^{-9}. The $^{233}U/^{236}U$ atomic ratios obtained vary from 0.12 × 10^{-2} to 1.16 × 10^{-2}, with the majority distributed in the range of (0.2 -0.7) × 10^{-2}.

We applied $^{233}U/^{236}U$ and $^{236}U/^{238}U$ atomic ratios in a binary mixing model to identify possible ^{236}U source terms. The results indicate that anthropogenic ^{236}U and ^{233}U in Greenland surface seawater originated from the direct global fallout (GF) and the Sellafield and La Hague reprocessing plants (RP) is diluted by a third endmember, mostly likely natural ocean water (NOW), containing marginal ^{236}U and ^{233}U. A preliminary estimation of the source terms of ^{236}U using the $^{233}U/^{236}U$ atomic ratio indicate that for both eastern and western Greenland seawater contributions from GF constitute about 30 % of ^{236}U. The dominating source for ^{236}U, i.e. 70 %, is associated to reactor ^{236}U including discharges from RP and local reactor input in the Arctic Ocean.

Keywords

^{233}U, ^{236}U, Greenland coast, surface seawater, 2012-2016

1. INTRODUCTION

Nuclear accidents (e.g., Chernobyl, Fukushima), weapons production and reprocessing plants (e.g., Sellafield (SF) in UK and La Hague (LH) in France) have released large amounts of man-made radioactive contaminants to the environment. Some radioisotopes (e.g., ^{3}H, ^{14}C, ^{134}Cs, ^{137}Cs, ^{129}I, ^{99}Tc) have relatively high mobility and bioavailability in oxic waters, making them valuable tracers in oceanographic studies (Hou et al., 2002; Karcher et al., 2004; Smith et al., 2011). In recent years, the long-lived minor uranium isotope ^{236}U ($T_{½}$= 2.34 ×10^{7} y) has been identified as an appealing new oceanographic tracer (Casacuberta et al., 2014; Christl et al., 2015, 2013, 2012; Eigl et al., 2013; Sakaguchi et al., 2012; Winkler et al., 2012) due to its superior properties including high solubility, long residence time (10^{5} y), and the well-understood steady circulation of natural uranium in the open ocean (Al-qasmi et al., 2016; Bellucci et al., 2013; Boulyga et al., 2002; Casacuberta et al., 2016; Chamizo et al., 2008; Desideri et al., 2002; Hotchkis et al., 2000; Lee et al., 2008; Parrish et al., 2006; Purser et al., 1996; Qiao et al., 2017; Quinto et al., 2009; Sakaguchi et al., 2016; Steier et al., 2008; Wendel et al., 2013; Winkler et al., 2012; Yang et al., 2016).

The Arctic is a key and most sensitive area of global climate change (Hansen et al., 2010), however, many processes in ocean circulation in the Arctic are poorly understood due to the lack of observations. The Arctic Ocean is surrounded by a disproportionally large continental shelf sea area into which several large rivers flow, supplying 10 % of the global river discharge (McClelland et al., 2012). The surface oceanic current, Greenland Current, is a combination of polar sea surface drift, return flow of the North Atlantic Current, and Irminger Current waters.The East Greenland Current (EGC) is of major importance because it directly connects the Arctic to the Northern Atlantic. The EGC is a major contributor to sea ice export out of the Arctic (Woodgate et al., 1999), and it is a major freshwater sink for the Arctic (Schlichtholz and Houssais, 1999).

Anthropogenic ^{236}U (>1000 kg) clearly dominates over its natural inventory (about 35 kg) in the environment, with the primary source terms including global fallout from atmospheric nuclear weapons testing (900-1400 kg) and discharges from reprocessing plants at SF and LH (115-250 kg) (Castrillejo et

al., 2020; Sakaguchi et al., 2009; Steier et al., 2008). Even though a growing set of ^{236}U data exists for the open oceans, reported ^{236}U data in the Arctic Ocean, especially in Greenland marine system are very limited (Castrillejo et al., 2018; Wefing et al., 2019). A good understanding of the input function of ^{236}U is critical for establishing it as a reliable tracer. However, the ^{236}U budget in the Atlantic-Arctic Ocean is still an open question due to incomplete records of the ^{236}U emission from SF and LH (Castrillejo et al., 2020; Christl et al., 2015, 2013).

Moreover, tracer studies using solely ^{236}U suffer from methodological difficulties to distinguish variations in ^{236}U source terms. Several studies have proposed the combination with other radionuclides, e.g. ^{129}I, to trace different water masses (Casacuberta et al., 2018, 2016; Castrillejo et al., 2018; Wefing et al., 2019). However, due to the different input functions and transport pathways of ^{129}I and ^{236}U, as well as different chemical-physical behaviour between these two elements, challenges in $^{236}U/^{129}I$ tracer applications are still encountered.

^{233}U ($T_{½}$= 1.59 ×10^5 y) is also an anthropogenic uranium trace isotope like ^{236}U. Different from $^{236}U/^{129}I$ ratios, $^{233}U/^{236}U$ ratios are unaffected by the environmental pathways. A recently published study demonstrated the high potential for $^{233}U/^{236}U$ to be used as a robust fingerprint to distinguish emission sources of anthropogenic U (Hain et al., 2020). ^{233}U was mostly produced during nuclear weapons testing by fast neutrons via ^{235}U (n, 3n) ^{233}U reactions or directly by ^{233}U-fueled devices, whereas almost no ^{233}U is produced in thermal nuclear power reactors or reprocessing plants (Hain et al., 2020). The representative $^{233}U/^{236}U$ atomic ratio was suggested to be $(1.40 \pm 0.12) \times 10^{-2}$ for global fallout. $^{233}U/^{236}U$ atomic ratios in LH discharges are at the level of 1×10^{-7}-1×10^{-6} (HELCOM MORS Discharge database), which is in good agreement with reactor model calculations obtained for the fuel of pressurized water reactors (Naegeli, 2004). In the Irish Sea, an average $^{233}U/^{236}U$ atomic ratio of $(0.12 \pm 0.01) \times 10^{-2}$ was measured (Hain et al., 2020).

In this work, we report data on $^{233}U/^{236}U$ in Greenland seawater for the first time and aim to draw a picture about the levels, distribution pattern and source terms of ^{236}U in Greenland marine environment thus to prompt the application of ^{236}U-^{233}U as paired-tracer system in oceanographic studies.

2. EXPERIMENTAL

2.1 Samples, standards, reagents and samples.

Sampling around the Greenland coastal line during 2012-2016 was carried out in collaboration with Greenland Institute of Natural Resources and National Institute of Aquatic Resources (DTU Aqua), Denmark. Fig. 1 gives an overview of sampling locations and the main surface current systems in the North Atlantic - Nordic Seas-Arctic Ocean (Aarkrog et al., 1999; Hou and Hou, 2012; Iosjpe et al., 2013; Pedersen et al., 2005). The details of the currents around Greenland coast, sample information as well as the overall analytical results obtained in this work (Table S-1 to S-4) are given in the supplementary information. All the samples (ca. 600 L of each) were surface seawater from a depth of about 5 m, which were pumped into big barrels and then taken for determination of ^{238}U by ICP-MS (50 mL), $^{236}U/^{238}U$ and $^{233}U/^{236}U$ by AMS (2-5 L) and other radionuclides (e.g., ^{99}Tc, results are not shown here) in the laboratory.

Uranium standard solution (1.000 g/L in 2 M HNO_3) was purchased from NIST (Gaithersburg, MD), which was used after dilution as a standard for the inductively coupled plasma mass spectrometry (ICP-MS) measurement to quantify ^{238}U in seawater. All reagents used in the experiment were of analytical reagent grade and prepared using ultra-pure water (18 MΩ·cm). UTEVA resin (100-150 μm particle size) was purchased from Triskem International, Bruz, France and packed in 2-mL Econo-Columns (0.7 cm i.d. × 5 cm length, Bio-Rad Laboratories Inc., Hercules, CA) for the chemical purification of uranium isotopes.

2.2 Analytical methods for determination of ^{238}U, ^{236}U, and ^{233}U.

^{238}U in the ocean is of natural origin and not related to anthropogenic emissions. The ^{238}U present in the water samples was used for the normalization of the detected ^{236}U and ^{233}U in order to take into account the chemical yield and the detection efficiency for U. The concentration of ^{238}U in seawater was directly

104 measured by triple-quadrupole ICP-MS (Agilent 8800 ICP-QQQ, Agilent technologies) after 50-folder
105 dilution. The ICP-QQQ instrument was equipped with a standard introduction system consisting of a
106 MicroMist nebulizer and a Scott-type double-pass spray chamber, together with a Ni sampler cone, Ni
107 skimmer cone and x-lens. The experimental details for the ^{238}U direct measurement have been given
108 elsewhere (Qiao and Xu, 2017). The combined uncertainty for ^{238}U is estimated to be 10 %, consisting of
109 statistical counting uncertainty of samples, standard and blank, dilution of samples and standards,
110 uncertainty of certified value of ^{238}U standard and matrix effect.

111 The sample preparation procedure for ^{233}U and ^{236}U determination in seawater is based on our previous
112 report (Qiao et al., 2015). In short, the seawater samples with a volume of 2-5 L were filtrated with filter
113 paper (Munktell 00K, particle retention 5-6 μm) to remove large particles and then acidified to pH 2 with
114 concentrated HNO_3. Purified $FeCl_3$ solution (0.05 g/mL of Fe) was added to a final Fe concentration of
115 0.1 g/L. The sample was vigorously stirred with air bubbling for 5-10 minutes in order to decompose
116 carbonate complexes. 10 % $NH_3 \cdot H_2O$ was slowly added to adjust the pH to 8-9 for the co-precipitation of
117 U with $Fe(OH)_3$. The precipitate was allowed to settle for 0.5-1 h in order to decant most of the
118 supernatant. The sample slurry was centrifuged at 4000 rpm for 5 minutes and the supernatant was
119 discarded. The final residue was dissolved with 15 mL of 3 M HNO_3 and the solution was loaded onto a
120 2-mL UTEVA column which was pre-conditioned with 20 mL of 3 M HNO_3. The UTEVA column was
121 rinsed with 40 mL of 3 M HNO_3, followed by 20 mL of 6 M HCl. Uranium absorbed on the column was
122 eluted with 10 mL of 0.025 M HCl. The flow rate for the chromatographic separation was controlled
123 manually to 1.0-1.5 mL/min.

124 1-3 mg of Fe (as $FeCl_3$ solution) was added to the U eluate, and the sample was adjusted to pH>9 with
125 ammonia to co-precipitate U with $Fe(OH)_3$. The precipitate was dried in an oven at 100 ºC and was then
126 baked in a furnace at 800 ºC for 12 hours so that the U is finally embedded in a Fe_2O_3 matrix. The sample
127 was pressed into aluminium sputter target holders for the AMS measurement of $^{236}U/^{238}U$ and $^{233}U/^{236}U$.
128 The AMS measurements were carried out at the 3-MV tandem accelerator facility VERA (Vienna
129 Environmental Research Accelerator) at the University of Vienna, Austria. The detailed method

for AMS measurements of ^{233}U and ^{236}U is reported elsewhere (Hain et al., 2020; Steier et al., 2019; Winkler et al., 2015).

2.3 Data quality control

For each batch of seven seawater samples, a process blank was prepared and analysed with respect to $^{236}U/^{238}U$ and $^{233}U/^{236}U$ ratios by AMS and ^{238}U concentration by ICP-MS, to monitor potential contaminations during the AMS measurement and the chemical sample preparation. Some process blanks showed occasionally elevated levels of ^{236}U and ^{233}U, which might be induced by the air-borne/particle-associated contamination from the ventilation system in the building (which has been worked with high radioactive waste samples from nuclear reactors). If the ^{236}U or ^{233}U count rate of the corresponding blank was more than 30 % of the respective sample, this sample including process blank was re-prepared, if possible, or rejected. For all the reported samples in this work, the blank level was taken into account in the uncertainties of the final measurement results, in some cases exceeding the uncertainty of the AMS measurement. The reference material IAEA-381 Irish seawater was analysed with respect to the $^{236}U/^{238}U$ ratio for quality assurance showing a very good agreement (i.e. error within ± 1σ) with the reference value (results are not shown here).

3. RESULTS AND DISCUSSION

3.1 ^{236}U concentration, $^{236}U/^{238}U$ and $^{233}U/^{236}U$ atomic ratios

The distributions of the detected ^{236}U concentrations and $^{236}U/^{238}U$ atomic ratios are presented graphically in Fig. 2 along with some published data for ^{236}U in the Arctic Ocean. The ^{238}U concentrations are in the range of 2.6-3.3 µg/L, show general positive correlation with salinity (Fig. S1). The low correlation coefficient (R^2=0.34) is attributed to the narrow distribution range and relatively high uncertainties (ca. 10%) in the ^{238}U results. The $^{236}U/^{238}U$ atomic ratios obtained vary within (1.1-15.5) × 10^{-9}, with majority of the results falling within (1.1-6.2) × 10^{-9}, which are up to 6 times higher than the estimated global fallout $^{236}U/^{238}U$ background level (1× 10^{-9}) in the open ocean surface (Christl et al., 2012). Two samples from 2013 (2013-0538 and 2013-0537) collected near the eastern Greenland coast

indicate much higher $^{236}U/^{238}U$ atomic ratios (8.5×10^{-9} and 15.5×10^{-9}, respectively). The ^{236}U concentrations vary within (0.7-12.9) $\times 10^7$ atom/L with majority in the range of (0.7-4.7) $\times 10^7$ atom/L. Again, the two above-mentioned samples show much higher ^{236}U concentrations (6.7×10^7 atom/L for 2013-0538 and 12.9×10^7 atom/L for 2013-0537, respectively). The validity of the ^{236}U measurements for these two samples (2013-0538 and 2013-0537) was confirmed by independently analysing 2-3 replicates for each sample.

$^{233}U/^{236}U$ atomic ratios obtained in this work vary from 0.12×10^{-2} to 1.16×10^{-2}, with the majority distributed in the range of (0.2 -0.7) $\times 10^{-2}$ (except 2013-0537 (0.12 ± 0.01) $\times 10^{-2}$ and 2012-0542 (1.16 ± 0.27) $\times 10^{-2}$) (Fig. 3). It is noteworthy that the sample (2013-0537) with the highest ^{236}U concentration shows the lowest $^{233}U/^{236}U$ atomic ratio (0.12 ± 0.01) $\times 10^{-2}$ among all samples collected in 2013 indicating a reactor signal of ^{236}U. The $^{233}U/^{236}U$ atomic ratio for the 2013-0538 sample of (0.68 ± 0.34) $\times 10^{-2}$ shows a high uncertainty (50 %) and therefore the obtained $^{233}U/^{236}U$ atomic ratio is excluded from interpretation.

The reported ^{236}U data in the Arctic region are limited. Casacuberta et al. (Casacuberta et al., 2016) observed ^{236}U ranging from 0.8×10^7 to 3.0×10^7 atom/L, with an average concentration of (2.3 ± 0.6) $\times 10^7$ atom/L for Arctic surface seawater in 2011-2012 (Casacuberta et al., 2016). Our results for ^{236}U concentrations in Greenland seawater in 2012 ((0.7-3.4) $\times 10^7$ atom/L, with an average of (1.9 ± 0.1) $\times 10^7$ atom/L) are comparable to their reported values. Our measured ^{236}U concentrations for 2015 ((1.2-3.1) $\times 10^7$ atom/L, with an average of (2.2 ± 0.6) $\times 10^7$ atom/L) also show good agreement with the observations by Casacuberta et al. (Casacuberta et al., 2018) for surface seawater from Barents Sea shelf, West Spitsbergen, Eurasian Basin and Makarov Basin collected in 2015 ((1.1-2.7) $\times 10^7$ atom/L, with an average of (1.6 ± 0.4) $\times 10^7$ atom/L). Wefing et al. (Wefing et al., 2019) reported ^{236}U concentrations of (1.2-2.2) $\times 10^7$ atom/L, with an average of (1.8 ± 0.3) $\times 10^7$ atom/L for samples from Fram Strait in 2016, which agree well with our results in 2016 ((0.8-2.0) $\times 10^7$ atom/L, with an average of (1.5 ± 0.4) $\times 10^7$ atom/L).

3.2 The time evolution and spatial distribution

3.2.1 Time evolution.

Box-plots of yearly ^{236}U concentration, as well as $^{236}U/^{238}U$ and $^{233}U/^{236}U$ atomic ratio for samples from East Greenland coast (EG) and West Greenland coast (WG) are shown in Fig. 4. The average of $^{236}U/^{238}U$ atomic ratios around the Greenland coast during 2012-2015 are at the level of (2-4) × 10^{-9}, with average ^{236}U concentrations varying within (1-3) × 10^{7} atom/L (Fig 4 (a)) and (b)). The highest mean values of $^{236}U/^{238}U$ atomic ratio and ^{236}U concentration for both EG and WG are observed in samples from 2013 even when the two samples (2013-0537, 0538) with elevated ^{236}U levels are excluded in the calculation.

It is noteworthy that larger variation of the $^{233}U/^{236}U$ atomic ratio appears in 2013 compared to the other years (Fig 4(c)). The appearance of high values in ^{236}U concentration in Greenlandic surface seawater in the year 2013 might be attributed to various reasons including 1) existence of additional source terms; 2) redistribution / remobilization of ^{236}U via water overflow, mixing and/or ice melting 3) enrichment of ^{236}U via biogeochemical processes, e.g., redox reaction or association to fine particles (e.g., colloid, nanoparticles). This is discussed later combing the quantitative estimation of ^{236}U source terms of Greenland seawater using $^{233}U/^{236}U$ atomic ratios.

Arctic climate change affects the distribution of radioactivity in the Arctic marine environment and the pathway of radionuclides (Karcher et al., 2010). Due to the high temperature in July 2012, strong melting across almost the entire surface of the Greenland ice sheet has been reported (Nghiem et al., 2012), as can be seen from the relatively low salinities in samples from 2012 (average 31.71± 1.86 ‰) compared to other years (Tables S1-S4). The ice melting might somehow dilute ^{236}U in the costal seawater in 2012, leading to relatively lower ^{236}U concentrations in the measured samples for 2012 compared to those for 2013.

3.2.2 Spatial distribution.

The ^{236}U concentration ((1.17 ± 0.13) × 10^{7} atom/L) in the seawater from the Faroe Islands (2016-0474) is comparable to the majority of the Greenland samples, which is in good agreement with previous findings for other radionuclides (Dahlgaard et al., 2004). Within our measurement uncertainties, no

206 significant difference in ^{236}U concentrations (as well as $^{236}U/^{238}U$ atomic ratios) between EG and WG
207 (Fig. 4) is obtained, which is supported by the statistical data analysis (VAR-3 (Vestergaard, 1964)). This
208 is in contrast to the distribution pattern of other radionuclides (e.g., ^{90}Sr, ^{137}Cs) reported earlier (Aarkrog
209 et al., 1999, 2000; Dahlgaard et al., 2004), where higher levels show up more often in the EG compared to
210 WG because radioactive discharges from SF and LH transported by Atlantic water firstly reach EG then
211 WG (Fig. 1 and Supplementary information).

212 Among the WG sampling stations, relatively high concentrations of ^{236}U are often observed at locations
213 around 64-67°N on west Greenland (e.g., samples of 2012-0535, 2013-0533, 2015-0508 and 2016-0511).
214 Upwelling phenomena have been reported at the west Greenland shelf between 64°N and 67°N (Pedersen
215 et al., 2005), which could potentially bring the subsurface water with higher ^{236}U concentration to the
216 surface water (Castrillejo et al., 2018). To better interpret the spatial distribution pattern of ^{236}U along the
217 Greenland coast, it is important to understand potential source terms of ^{236}U and ^{233}U in this region.

218 ### 3.3 Source terms of ^{236}U and ^{233}U around the Greenland coast

219 The overall sources of ^{236}U and ^{233}U in the Greenland coast seawater can be generally categorized in
220 two groups: 1) Global fallout (GF), including direct deposition of fallout from atmospheric weapons
221 testing into the ocean and indirect input via advective ocean water movement or via fresh water input
222 transporting GF signal from terrestrial area. 2) Reactor input (RT), including both discharges from
223 reprocessing plants (e.g., SF and LH) and regulatory/accidental releases from nuclear facilities (e.g. local
224 input in the Arctic).

225 #### 3.3.1 Global fallout.

226 The distribution of global fallout ^{236}U is dominating (70 %) in the Northern hemisphere and variable
227 with latitude (Aoyama et al., 2006). A $^{236}U/^{238}U$ atomic ratio of about 1×10^{-9} (corresponding to 0.8×10^{7}
228 atom/L when apply a typical ^{238}U concentration of 3.3 µg/L) to has been estimated for the global fallout
229 signature in modern ocean surface waters (Casacuberta et al., 2016; Christl et al., 2012). This agrees with
230 published measurement (0.85×10^{7} atom/L) on Northwest Pacific surface seawater (in 2014) where the
231 global fallout is the dominating source (Nomura et al., 2017a). Our results on average ^{236}U concentrations

((1.5-3.8) × 10^7 atom/L) over 2012-2016 are 2-4 times higher than the global fallout value, indicating additional input from other sources beside global fallout.

As mentioned earlier that ^{233}U can only be produced during nuclear weapons testing, therefore, global fallout is the major source of ^{233}U in the Greenland coast. The average $^{233}U/^{236}U$ atomic ratio for global fallout was obtained as (1.40 ± 0.12) × 10^{-2} (Hain et al., 2020) and we believe this value would stay constant in the open ocean with the termination of nuclear weapons test since 1980s. Therefore, any actual $^{233}U/^{236}U$ atomic ratios below (1.40 ± 0.12) × 10^{-2} for samples in the Greenland coast would indicate the admixing of reactor-associated ^{236}U in the marine system.

Global fallout ^{236}U and ^{233}U deposited on the catchment of Greenland and the ice sheet can also be transferred to the Greenlandic marine environment through freshwater input via river runoff and ice sheet melting (Aarkrog, 1994; Dickson et al., 2007). The Greenland ice sheet is the largest freshwater reservoir in the northern hemisphere with estimated annual fresh water flux in the range of 0.3-0.7 km^3/y (Dickson et al., 2007). Wendel et al. (Wendel et al., 2013) have reported $^{236}U/^{238}U$ atomic ratios of (4 -100) × 10^{-6} in an Arctic ice core. Lower salinity samples (< 30 ‰) measured in this work seem not associate to high ^{236}U concentrations (Fig. S1), indicating the indirect transport of global fallout ^{236}U (and ^{233}U) via river/melt water is not significant.

3.3.2 Reactor input

Reprocessing plants of SF and LH. Most of the radioactive emissions from LH were transported through the English Channel to the North Sea, while those from SF flow mostly north around the Scottish coastline and then into the North Sea. The newly reconstructed ^{236}U release history from SF and LH show a general decreasing trend since 1970s (Fig. S2) (Castrillejo et al., 2020). The $^{236}U/^{238}U$ atomic ratios obtained in this work are several folders lower compared to those reported for the open North Sea, but higher than other open oceans which mainly receive ^{236}U from global fallout, such as Equatorial Atlantic Ocean, Sea of Japan and Northwest pacific Ocean (Casacuberta et al., 2014; Nomura et al., 2017b;

Sakaguchi et al., 2012). This is in accordance with our expectation that discharges from the two major European nuclear reprocessing plants are important sources of ^{236}U in Greenlandic seawater.

From the North Sea, the reprocessing ^{236}U can be transported to the Greenland coast by two ways: 1) northward transport via the Norwegian Coastal Current (NCC) and partly the Norwegian Atlantic Current (NAC) to Arctic Ocean and back from the Arctic Ocean via EGC; 2) The second branch of the NAC turning back at Fram Strait and westward to Greenland merging into EGC (Raisbeck et al., 1995). These two branches are further sub-divided into several loops in the Arctic ocean with different transit times (Karcher et al., 2004; Smith et al., 2011).

Local input. A number of potential local sources for anthropogenic radionuclides in the Arctic region have been reported, including radioactive waste dumping and submarine accidents (e.g., Komsomolets) from USSR (Nies et al., 1999, 1998; Yablokov, 2001), close-in fallout from Novaya Zemlya nuclear weapon test site (Aarkrog, 1994; Nies et al., 1998), Siberian river discharge and other operational emission (Aarkrog, 1994; Karcher et al., 2010), nuclear powered satellite (Cosmos 954) accident (Grasty, 1995; Taylor et al., 1979; U.S Department of Energy, 1978), normal or accidental releases from Chalk River labs (Cross, 1980) and contaminants from the Chernobyl accident (Davidson et al., 1987). However, in terms of ^{236}U and ^{233}U inventories in these sources, nearly no documentation is available. The only report for Cosmos 954 indicated that the nuclear reactor aboard was estimated to contain about 50 kg of highly enriched ^{235}U (U.S Department of Energy, 1978), which would have potentially produced ^{236}U via the (n,γ)-reaction. However, due to limitations in the available measurement techniques applied in radiological surveys after the accident, no data on ^{236}U concentration have been reported. Therefore, it is apparent that further investigation is necessary to clarify all the above-mentioned local source terms in the Arctic.

3.4 Application of the $^{233}U/^{236}U$ ratio and binary mixing model for ^{236}U source identification

All measured $^{236}U/^{238}U$ and $^{233}U/^{236}U$ atomic ratios are plotted in a diagram (Fig. 5) demonstrating the binary mixing of the direct global fallout (DGF) and reprocessing plants of SF and LH (RP. The detailed parameters of the end-members are summarized in Table S5.

It can been seen from Fig. 5 that most of our observation data are below the binary mixing line of DGF and RP, indicating the existence of an extra endmember featured with relative low atomic ratios for both $^{233}U/^{236}U$ and $^{236}U/^{238}U$. This endmember in the mixing diagram is mostly likely natural ocean water (NOW) containing neither anthropogenic ^{236}U nor ^{233}U. The deviation from the mixing line gives the dilution of water from the two endmembers DGF and LH by the endmember NOW. In principle, any water less affected by anthropogenic U (and essentially any deep water) will lead to this dilution.

3.5 Quantitative estimation of the ^{236}U source term based on $^{233}U/^{236}U$ atomic ratios

A preliminary estimation is made to quantitatively evaluate the ^{236}U contribution from GF and RT as above-defined, based on $^{233}U/^{236}U$ atomic ratios using the following equation.

$$R_s = \frac{N_{233,f} + N_{233,r}}{N_{236,f} + N_{236,r}} = \frac{N_{236,f} \cdot R_f + N_{236,r} \cdot R_r}{N_{236,f} + N_{236,r}} = \frac{N_{233,f}/N_{236,r} R_f + R_r}{N_{236,f}/N_{236,r} + 1} \quad (1)$$

Where R_s, R_f and R_r respectively represent the $^{233}U/^{236}U$ atomic ratio of the Greenlandic seawater, global fallout and nuclear reactor; $N_{233,f}$ and $N_{233,r}$ refer to the atomic number of ^{233}U from global fallout and reactor, respectively; $N_{236,f}$ and $N_{236,r}$ refer to the atomic number of ^{236}U from global fallout and reactor, respectively. Therefore, the proportion (P_f) of GF can be obtained using equation (2).

$$P_f, \% = \frac{N_{236,f}}{N_{236,r\,+\,N_{236,f}}} = \frac{R_s - R_r}{R_f - R_r} \quad (2)$$

Assuming R_r = 1.4 × 10^{-2} and R_r =1 × 10^{-6}, the calculation results in Table 1 indicate that ^{236}U in Greenland seawater consists of (29 ± 5) % from GF and (29 ±9) % from RT in both EG and WG. The GF contributions obtained here are comparable to the values calculated using representative global fallout ^{236}U concentration of 0.8 × 10^7 atom/L divided by the mean ^{236}U concentration measured in this work,

which are (32 ± 12) % for EG and (26 ±7) % for WG, respectively. This indicates high proportion (about 70 %)) of ^{236}U in Greenlandic surface seawater is associated to a reactor signal. A semi-quantitative estimation based on transfer time and transit time (see detailed calculation in supplementary information) shows that the contribution from RP is (49 ± 21) % for EG and (33 ± 4) % for WG during 2011-2016, the remaining reactor contribution (e.g., local input) is obtained as (7 ± 15) % for EG and (38 ± 14) % for WG (Table S5). To better quantify the contribution of reactor ^{236}U from RP and local input from the Arctic, a more realistic oceanic model (e.g., transit time distribution (TTD)) is necessary (Smith et al., 2011).

We further calculated the ^{236}U concentration associated to a reactor signal for each sample by subtracting the global fallout contribution and plotted the residue (i.e., reactor ^{236}U) along the longitude belt in Fig. 6. A higher reactor ^{236}U signal is observed in 2013, compared to the years before and after. It seems unlikely that this additional input is related to the variation of SF and LH discharges (Fig. S2), because this higher ^{236}U level is only observed within in narrow latitude/longitude belt (61-65 °N, 36-40 °W). It might be connected to local changes in ocean current branches, which potentially brought more SF and LH water to the southeast of Greenland in 2013. The much higher ^{236}U level in sample 2013-0537 seems to be an exception and is difficult to explain in an oceanographic context. To reveal the origin and the transport pathway of this additional reactor ^{236}U input further investigations are needed.

CONCLUSIONS

A first dataset of ^{236}U and ^{233}U in the Greenland marine environment during the 5-year period (2012-2016) is reported. ^{236}U concentrations obtained for the Greenland surface seawater are distributed within a relatively narrow range, with average ^{236}U concentrations being 2-4 times higher than the estimated value from direct global fallout. Contrary to the spatial distribution pattern of other radionuclides (e.g., ^{137}Cs and ^{90}Sr) reported earlier, we do not observe a significant difference in ^{236}U concentration between the east and west Greenland coast, which is supported by the statistical data analysis (VAR-3). Application of a binary mixing model to the correlation between $^{233}U/^{236}U$ and $^{236}U/^{238}U$ atomic ratios indicates that ^{236}U contributed from the direct global fallout and the SF and LH reprocessing plants is diluted by a third

endmember (mostly likely natural ocean seawater) with marginal anthropogenic ^{236}U and ^{233}U. A preliminary estimation of the ^{236}U source term composition using $^{233}U/^{236}U$ atomic ratios indicate that global fallout contributes only about 30 %, while the majority (about 70 %) of ^{236}U is associated to nuclear reactor signal in Greenland coastal water. Further investigation with focus on the analysis of ^{233}U and ^{236}U in deep Greenlandic seawater is necessary to clarify the transport pathway and further use ^{236}U-^{233}U as paired-tracer system to identify different water masses.

ACKNOWLEDGEMENT

J. Qiao is grateful to support from colleagues in the Radioecology and Tracer Studies, Department of Environmental Engineering, Technical University of Denmark and Professor Robin Gloser at VERA, University of Vienna. The authors also wish to thank the Environmental Protection Agency, Danish Ministry of the Environment, for financial support, and the Greenland Institute for Natural resources and the National Institute for Aquatic Resources, DTU Aqua, for collecting seawater samples from Greenland.

REFERENCES

Aarkrog, a., Dahlgaard, H., Nielsen, S.P., 1999. Marine radioactivity in the Arctic: A retrospect of environmental studies in Greenland waters with emphasis on transport of 90Sr and 137Cs with the East Greenland Current. Sci. Total Environ. 237–238, 143–151. https://doi.org/10.1016/S0048-9697(99)00131-X

Aarkrog, A., 1994. Radioactivity in polar regions - Main sources. J. Environ. Radioact. 25, 21–35. https://doi.org/10.1016/0265-931X(94)90005-1

Aarkrog, A., Dahlgaard, H., Nielsen, S.P., 2000. Environmental radioactive contamination in Greenland: a 35 years retrospect. Sci. Total Environ. 245, 233–248. https://doi.org/10.1016/s0048-9697(99)00448-9

Al-qasmi, H., Law, G.T.W., Fi, L.K., Livens, F.R., 2016. Origin of artificial radionuclides in soil and sediment from North Wales. J. Environ. Radioact. 151, 244–249. https://doi.org/10.1016/j.jenvrad.2015.10.013

Aoyama, M., Hirose, K., Igarashi, Y., 2006. Re-construction and updating our understanding on the global weapons tests137Cs fallout. J. Environ. Monit. 8, 431–438. https://doi.org/10.1039/b512601k

Bellucci, J.J., Simonetti, A., Wallace, C., Koeman, E.C., Burns, P.C., 2013. Isotopic Fingerprinting of the World's First Nuclear Device Using Post-Detonation Materials. Anal. Chem. 85, 4195–4198. https://doi.org/10.1021/ac400577p

Boulyga, S.F., Matusevich, J.L., Mironov, V.P., Kudrjashov, V.P., Halicz, L., Segal, I., McLean, J.A., Montaser, A., Sabine Becker, J., 2002. Determination of 236U/238U isotope ratio in contaminated environmental samples using different ICP-MS instruments. J. Anal. At. Spectrom. 17, 958–964.

Casacuberta, N., Christl, M., Lachner, J., van der Loeff, M.R., Masqué, P., Synal, H. a., 2014. A first transect of 236U in the North Atlantic Ocean. Geochim. Cosmochim. Acta 133, 34–46. https://doi.org/10.1016/j.gca.2014.02.012

Casacuberta, N., Christl, M., Vockenhuber, C., Wefing, A.M., Wacker, L., Masqué, P., Synal, H.A., Rutgers van der Loeff, M., 2018. Tracing the Three Atlantic Branches Entering the Arctic Ocean With 129I and 236U. J. Geophys. Res. Ocean. 123, 6909–6921. https://doi.org/10.1029/2018JC014168

Casacuberta, N., Masqué, P., Henderson, G., Rutgers van-der-Loeff, M., Bauch, D., Vockenhuber, C., Daraoui, A., Walther, C., Synal, H.A., Christl, M., 2016. First 236U data from the Arctic Ocean and use of 236U/238U and 129I/236U as a new dual tracer. Earth Planet. Sci. Lett. 440, 127–134. https://doi.org/10.1016/j.epsl.2016.02.020

Castrillejo, M., Casacuberta, N., Christl, M., Vockenhuber, C., Synal, H.-A., García-Ibáñez, M.I., Lherminier, P., Sarthou, G., Garcia-Orellana, J., Masqué, P., 2018. Tracing water masses with 129I and 236U in the subpolar North Atlantic along the GEOTRACES GA01 section. Biogeosciences Discuss. 1–28. https://doi.org/10.5194/bg-2018-228

Castrillejo, M., Witbaard, R., Casacuberta, N., Richardson, C.A., Dekker, R., Synal, H.A., Christl, M., 2020. Unravelling 5 decades of anthropogenic 236U discharge from nuclear reprocessing plants. Sci. Total Environ. 717, 137094. https://doi.org/10.1016/j.scitotenv.2020.137094

Chamizo, E., Jimenez-Ramos, M., Wacker, L., Vioque, I., Calleja, A., Garcia-Leon, M., Garcia-Tenorio, R., 2008. Isolation of Pu-isotopes from environmental samples using ion chromatography for accelerator mass spectrometry and alpha spectrometry. Anal. Chim. Acta 606, 239–245.

385 Christl, M., Casacuberta, N., Lachner, J., Maxeiner, S., Vockenhuber, C., Synal, H.-A., Goroncy,
386 I., Herrmann, J.J., Daraoui, A., Walther, C., Michel, R., 2015. Status of 236U analyses at
387 ETH Zurich and the distribution of 236U and 129I in the North Sea in 2009. Nucl. Instr.
388 Meth. Phys. Res. BMeth. 361, 510–516. https://doi.org/10.1016/j.nimb.2015.01.005
389 Christl, M., Lachner, J., Vockenhuber, C., Goroncy, I., Herrmann, J.J., Synal, H.-A., 2013. First
390 data of Uranium-236 in the North Sea. Nucl. Instr. Meth. B 294, 530–536.
391 https://doi.org/10.1016/j.nimb.2012.07.043
392 Christl, M., Lachner, J., Vockenhuber, C., Lechtenfeld, O., Stimac, I., van der Loeff, M.R.,
393 Synal, H.-A., 2012. A depth profile of uranium-236 in the Atlantic Ocean. Geochim.
394 Cosmochim. Acta 77, 98–107. https://doi.org/10.1016/j.gca.2011.11.009
395 Cross, W.G., 1980. The Chalk River accident in 1952, PAM/0089/1980.
396 Dahlgaard, H., Eriksson, M., Nielsen, S.P., Joensen, H.P., 2004. Levels and trends of radioactive
397 contaminants in the Greenland environment. Sci. Total Environ. 331, 53–67.
398 https://doi.org/10.1016/j.scitotenv.2004.03.023 ER
399 Davidson, A.C.I., Harrington, J.R., Stephenson, M.J., Monaghan, M.C., Schell, W.R., 1987.
400 Radioactive Cesium from the Chernobyl Accident in the Greenland Ice Sheet. Science (80-.
401). 237, 633–634.
402 Desideri, D., Meli, M. a, Roselli, C., Testa, C., Boulyga, S.F., Becker, J.S., 2002. Determination
403 of 236U and transuranium elements in depleted uranium ammunition by alpha-spectrometry
404 and ICP-MS. Anal. Bioanal. Chem. 374, 1091–5. https://doi.org/10.1007/s00216-002-1575-
405 5
406 Dickson, R., Rudels, B., Dye, S., Karcher, M., Meincke, J., Yashayaev, I., 2007. Current
407 estimates of freshwater flux through Arctic and subarctic seas. Prog. Oceanogr. 73, 210–

230. https://doi.org/10.1016/j.pocean.2006.12.003

Eigl, R., Srncik, M., Steier, P., Wallner, G., 2013. 236U/238U and 240Pu/239Pu isotopic ratios in small (2 L) sea and river water samples. J. Environ. Radioact. 116, 54–58.

Grasty, R.L., 1995. Environmental monitoring by airborne gamma ray spectrometry, experience at the Geological Survey of Canada, IAEA-TECDOC-827.

Hain, K., Steier, P., Froehlich, M.B., Golser, R., Hou, X., Lachner, J., Qiao, J., Quinto, F., Sakaguchi, A., 2020. 233U/236U signature allows to distinguish environmental emissions of civil nuclear industry from weapons fallout. Nat. Commun. 11. https://doi.org/https://doi.org/10.1038/s41467-020-15008-2

Hansen, J., Ruedy, R., Sato, M., Lo, K., 2010. Global surface temperature change. Rev. Geophys. 48, 1–29. https://doi.org/10.1029/2010RG000345

HELCOM MORS Discharge database [WWW Document], n.d. URL https://helcom.fi/baltic-sea-trends/data-maps/databases/ (accessed 5.20.20).

Hotchkis, M.A.C., Child, D., Fink, D., Jacobsen, G.E., Lee, P.J., Mino, N., Smith, A.M., Tuniz, C., 2000. Measurement of 236U in environmental media. Nucl. Instruments Methods Phys Res - Sect. B Only - Beam Interact Mater Atoms 172, 659–665.

Hou, X., Hou, Y., 2012. Analysis of 129I and its Application as Environmental Tracer. J. Anal. Sci. Technol. 3, 135–153. https://doi.org/10.5355/JAST.2012.135

Hou, X.L., Dahlgaard, H., Nielsen, S.P., Kucera, J., 2002. Level and origin of Iodine-129 in the Baltic Sea. J. Environ. Radioact. 61, 331–343.

Iosjpe, M., Isaksson, M., Joensen, H.P., Lahtinen, J., Logemann, K., Pálsson, S.E., Roos, P., Suolanen, V., 2013. Consequences of severe radioactive releases to Nordic Marine environment. Nordic nuclear safety research, NKS-276.

Karcher, M., Harms, I., Standring, W.J.F., Dowdall, M., Strand, P., 2010. On the potential for climate change impacts on marine anthropogenic radioactivity in the Arctic regions. Mar. Pollut. Bull. 60, 1151–9. https://doi.org/10.1016/j.marpolbul.2010.05.003

Karcher, M.J., Gerland, S., Harms, I.H., Iosjpe, M., Heldal, H.E., Kershaw, P.J., Sickel, M., 2004. The dispersion of 99Tc in the Nordic Seas and the Arctic Ocean: A comparison of model results and observations. J. Environ. Radioact. 74, 185–198. https://doi.org/10.1016/j.jenvrad.2004.01.026

Lee, S.H., Povinec, P.P., Wyse, E., Hotchkis, M.A.C., 2008. Ultra-low-level determination of 236U in IAEA marine reference materials by ICPMS and AMS. Appl. Radiat. Isot. 66, 823–828.

McClelland, J.W., Holmes, R.M., Dunton, K.H., Macdonald, R.W., 2012. The Arctic Ocean Estuary. Estuaries and Coasts 35, 353–368. https://doi.org/10.1007/s12237-010-9357-3

Naegeli, R.E., 2004. Calculation of the Radionuclides in PWR Spent Fuel Samples for SFR Experiment Planning, Sandia National Laboratories. Technical Report, Sandia National Laboratories, Albuquerque, NM 87123, USA.

Nghiem, S. V., Hall, D.K., Mote, T.L., Tedesco, M., Albert, M.R., Keegan, K., Shuman, C.A., DiGirolamo, N.E., Neumann, G., 2012. The extreme melt across the Greenland ice sheet in 2012. Geophys. Res. Lett. 39, 6–11. https://doi.org/10.1029/2012GL053611

Nies, H., Harms, I.H., Karcher, M.J., Dethleff, D., Bahe, C., 1999. Anthropogenic radioactivity in the Arctic Ocean - Review of the results from the joint German project. Sci. Total Environ. 237–238, 181–191. https://doi.org/10.1016/S0048-9697(99)00134-5

Nies, H., Harms, I.H., Karcher, M.J., Dethleff, D., Bahe, C., Kuhlmann, G., Oberhuber, J.M., 1998. Anthropogenic Radioactivity in the Nordic Seas and the Arctic Oc ean - Results of a

Joint Project. Ger. J. Hydrogr. 50, 313–343.

Nomura, T., Sakaguchi, A., Steier, P., Eigl, R., Yamakawa, A., Watanabe, Takaaki, Sasaki, K., Watanabe, Tsuyoshi, Golser, R., Takahashi, Y., Yamano, H., 2017a. Reconstruction of the temporal distribution of236U/238U in the Northwest Pacific Ocean using a coral core sample from the Kuroshio Current area. Mar. Chem. 190, 28–34. https://doi.org/10.1016/j.marchem.2016.12.008

Nomura, T., Sakaguchi, A., Steier, P., Eigl, R., Yamakawa, A., Watanabe, Takaaki, Sasaki, K., Watanabe, Tsuyoshi, Golser, R., Takahashi, Y., Yamano, H., 2017b. Reconstruction of the temporal distribution of236U/238U in the Northwest Pacific Ocean using a coral core sample from the Kuroshio Current area. Mar. Chem. 190, 28–34. https://doi.org/10.1016/j.marchem.2016.12.008

Parrish, R., Thirlwall, M., Pickford, C., Horstwood, M., Gerdes, A., Anderson, J., Coggon, D., 2006. Determinaiton of 238U/235U, 236U/238U and uramium concentraiton in urine using SF-ICP-MS and MC-ICP-MS: na interlaboratory comparison. Health Phys. 90, 127–138.

Pedersen, S. a., Ribergaard, M.H., Simonsen, C.S., 2005. Micro- and mesozooplankton in Southwest Greenland waters in relation to environmental factors. J. Mar. Syst. 56, 85–112. https://doi.org/10.1016/j.jmarsys.2004.11.004

Purser, K.H., Kilius, L.R., Litherland, A.E., Zhao, X., 1996. Detection of 236U: a possible 100-million year neutron flux integrator. Nucl. Instruments Methods Phys. Res. Sect. B Beam Interact. with Mater. Atoms 113, 445–452. https://doi.org/10.1016/0168-583X(95)01369-5

Qiao, J., Hou, X., Steier, P., Nielsen, S., Golser, R., 2015. Method for 236U Determination in Seawater Using Flow Injection Extraction Chromatography and Accelerator Mass Spectrometry. Anal. Chem. 87, 7411–7417.

Qiao, J., Steier, P., Nielsen, S., Hou, X., Roos, P., Golser, R., 2017. Anthropogenic 236U in Danish seawater: global fallout versus reprocessing discharge. Environ. Sci. Technol. 51, 6867–6876. https://doi.org/10.1021/acs.est.7b00504

Qiao, J., Xu, Y., 2017. Direct measruement of uranium in seawater by inductively coupled mass spectrometry.

Quinto, F., Steier, P., Wallner, G., Wallner, A., Srncik, M., Bichler, M., Kutschera, W., Terrasi, F., Petraglia, A., Sabbarese, C., 2009. The first use of 236U in the general environment and near a shutdown nuclear power plant. Appl. Radiat. Isot. 67, 1775–1780.

Raisbeck, G.M., Yiou, F., Zhou, Z.Q., Kilius, L.R., 1995. 129I from nuclear fuel reprocessing facilities at Sellafield (U.K.) and La Hague (France); potential as an oceanographie tracer. J. Mar. Syst. 6, 561–570. https://doi.org/10.1016/0924-7963(95)00024-J

Sakaguchi, A., Kadokura, A., Steier, P., Takahashi, Y., Shizuma, K., Hoshi, M., Nakakuki, T., Yamamoto, M., 2012. Uranium-236 as a new oceanic tracer: A first depth profile in the Japan Sea and comparison with caesium-137. Earth Planet. Sci. Lett. 333, 165–170. https://doi.org/10.1016/j.epsl.2012.04.004

Sakaguchi, A., Kawai, K., Steier, P., Quinto, F., Mino, K., Tomita, J., Hoshi, M., Whitehead, N., Yamamoto, M., 2009. First results on 236U levels in global fallout. Sci. Total Environ. 407, 4238–4242. https://doi.org/10.1016/j.scitotenv.2009.01.058

Sakaguchi, A., Nomura, T., Steier, P., Gloser, R., Sasaki, K., Watanabe, T., Nakakuki, T., Takahashi, Y., Yamano, H., 2016. Temporal and vertical distributions of anthropogenic 236U in the Japan Sea using a coral core and seawater samples. J. Geophys. Res. Ocean. 121, 4–13. https://doi.org/10.1002/2015JC011109

Schlichtholz, P., Houssais, M.N., 1999. An investigation of the dynamics of the East Greenland

Current in Fram Strait based on a simple analytical model. J. Phys. Oceanogr. 29, 2240–2265. https://doi.org/10.1175/1520-0485(1999)029<2240:AIOTDO>2.0.CO;2

Smith, J.N., McLaughlin, F. a., Smethie, W.M., Moran, S.B., Lepore, K., 2011. Iodine-129, 137Cs, and CFC-11 tracer transit time distributions in the Arctic Ocean. J. Geophys. Res. Ocean. 116, 1–19. https://doi.org/10.1029/2010JC006471

Steier, P., Bichler, M., Keith Fifield, L., Golser, R., Kutschera, W., Priller, A., Quinto, F., Richter, S., Srncik, M., Terrasi, P., Wacker, L., Wallner, A., Wallner, G., Wilcken, K.M., Maria Wild, E., 2008. Natural and anthropogenic 236U in environmental samples. Nucl. Inst.and Methods Phys. Res. B 266, 2246–2250.

Steier, P., Hain, K., Klötzli, U., Lachner, J., Priller, A., Winkler, S., Golser, R., 2019. The actinide beamline at VERA. Nucl. Instruments Methods Phys. Res. Sect. B Beam Interact. with Mater. Atoms 458, 82–89. https://doi.org/10.1016/j.nimb.2019.07.031

Taylor, H.W., Hutchison, E.A., Mcinnes, K.L., Svoboda, J., 1979. Cosmos 954 - Search for Airborne Radioactivity on Lichens in the Crash Area, Northwest-Territories, Canada. Science (80-.). 205, 1383–1385.

U.S Department of Energy, 1978. Operation Morning Light, Northwest Territories, Canada-1987, A non-technical summary of U.S. participation.

Vestergaard, J., 1964. Analysis of variance with unequal numbers in groups. Gier system library no. 211. Copenhagen.

Wefing, A.M., Christl, M., Vockenhuber, C., Rutgers van der Loeff, M., Casacuberta, N., 2019. Tracing Atlantic Waters Using 129 I and 236 U in the Fram Strait in 2016. J. Geophys. Res. Ocean. 124, 882–896. https://doi.org/10.1029/2018JC014399

Wendel, C.C., Oughton, D.H., Lind, O.C., Skipperud, L., Fifield, L.K., Isaksson, E., Tims, S.G.,

523 Salbu, B., 2013. Chronology of Pu isotopes and 236U in an Arctic ice core. Sci. Total
524 Environ. 461–462, 734–741. https://doi.org/10.1016/j.scitotenv.2013.05.054
525 Winkler, S.R., Steier, P., Buchriegler, J., Lachner, J., Pitters, J., Priller, A., Golser, R., 2015. He
526 stripping for AMS of 236U and other actinides using a 3 MV tandem accelerator. Nucl.
527 Instruments Methods Phys. Res. Sect. B Beam Interact. with Mater. Atoms 361, 458–464.
528 https://doi.org/10.1016/j.nimb.2015.04.029
529 Winkler, S.R., Steier, P., Carilli, J., 2012. Bomb fall-out 236U as a global oceanic tracer using an
530 annually resolved coral core. Earth Planet. Sci. Lett. 359–360, 124–130.
531 Woodgate, R.A., Fahrbach, E., Rohardt, G., 1999. Structure and transports of the East Greenland
532 Current at 75°N from moored current meters. J. Geophys. Res. Ocean. 104, 18059–18072.
533 https://doi.org/10.1029/1999jc900146
534 Yablokov, A. V., 2001. Radioactive waste disposal in seas adjacent to the territory of the Russian
535 Federation. Mar. Pollut. Bull. 43, 8–18. https://doi.org/10.1016/S0025-326X(01)00073-X
536 Yang, G., Tazoe, H., Yamada, M., 2016. Analytica Chimica Acta Determination of 236U in
537 environmental samples by single extraction chromatography coupled to triple-quadrupole
538 inductively coupled plasma-mass spectrometry. Anal. Chim. Acta 944, 44–50.
539 https://doi.org/10.1016/j.aca.2016.09.033
540

Table 1. Estimation of ^{236}U source composition in Greenlandic seawater by $^{233}U/^{236}U$ ratios

Year	Average $^{233}U/^{236}U$ atomic ratio, × 10^{-2}		Contribution of GF, %*		Contribution of RT, %	
	EG	WG	EG	WG	EG	WG
2012	0.37 ± 0.07	NA	26 ± 4	NA	74 ± 4	NA
2013	0.42 ± 0.38	0.33 ± 0.14	30 ± 3	24 ± 5	70 ± 3	76 ± 5
2015	0.50 ± 0.09	0.35 ± 0.10	36 ± 2	25 ± 5	64 ± 2	75 ± 5
2016	0.33 ± 0.05	0.56 ± 0.11	23 ± 5	40 ± 2	77 ± 5	60 ± 2
Mean ± sd			29 ± 5	29 ± 9	71 ± 5	71 ± 9

*The value was calculated based on equation (2), with $R_r = 1.4 \times 10^{-2}$ and $R_r = 1 \times 10^{-6}$.

Figure 1. Map of Greenland coast showing the sampling locations (a) and general pattern of surface water currents (b). Blue arrows represent cold water currents, red arrows represent warm water currents and green arrows represent coastal water currents. NAC-Norwegian Atlantic Current, NCC-Norwegian Coastal Current, EGC-East Greenland Current, WSC-West Spitsbergen Current, WGC-Western Greenland Current, LH-La Hague nuclear reprocessing plant, SF-Sellafield nuclear reprocessing plant, FS-Faroe islands.

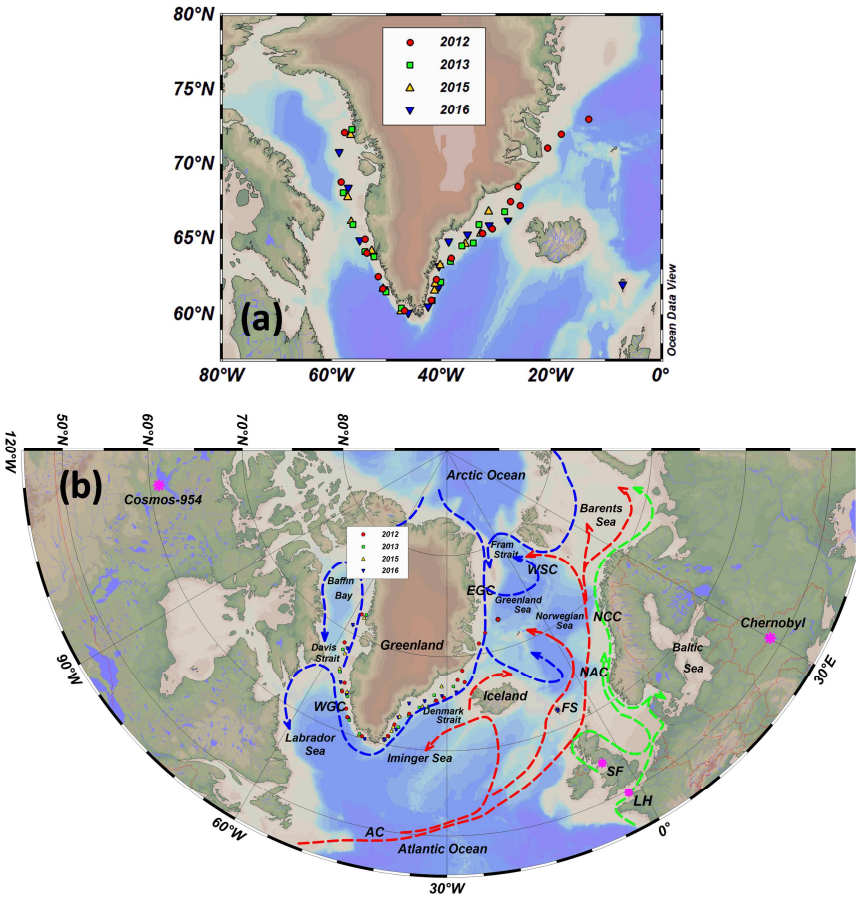

Figure 2. Time evolution and spatial distribution of ^{236}U concentration (left) and $^{236}U/^{238}U$ atomic ratio (right) in seawater around Greenland coast during 2012-2016. (Ref. a: Casacuberta et al. 2016; Ref. b: Casacuberta et al. 2018; Ref. c: Wefing et al. 2019)

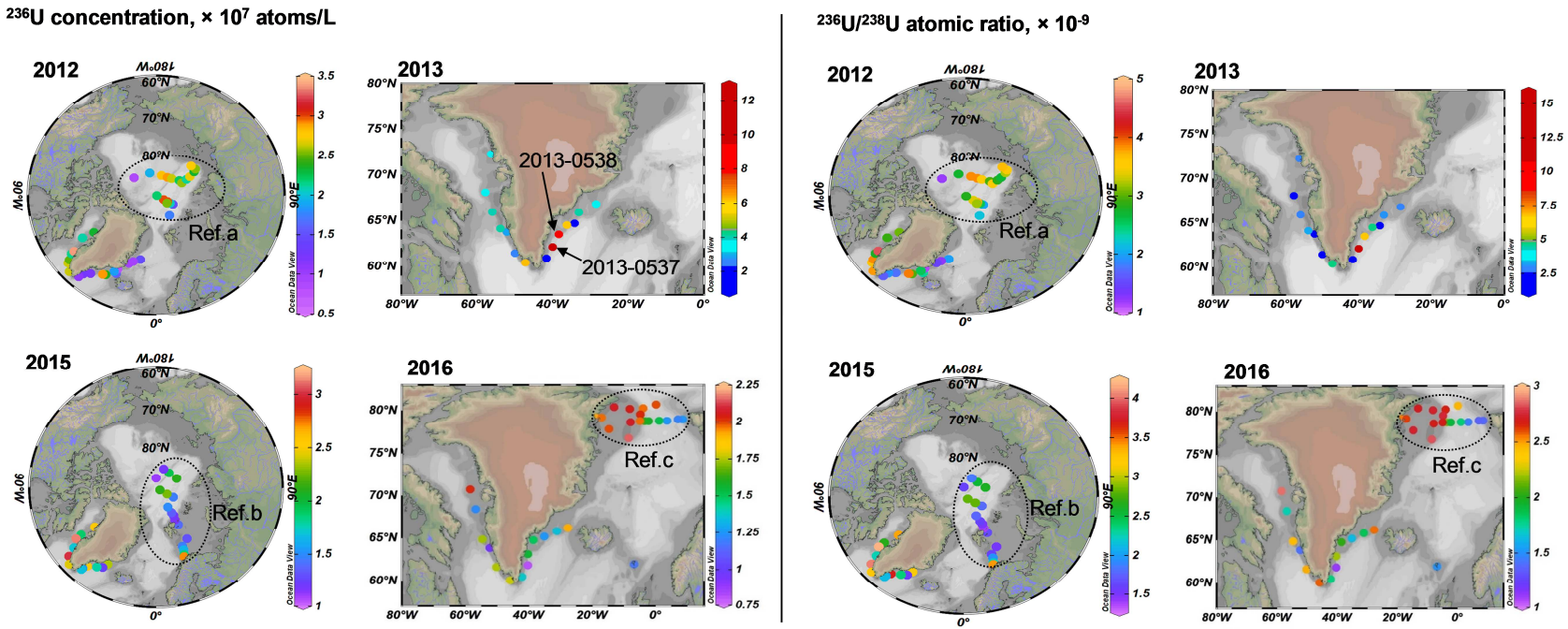

Figure 3. Time evolution and spatial distribution of $^{233}U/^{236}U$ atomic ratio in seawater around Greenland coast during 2012-2016.

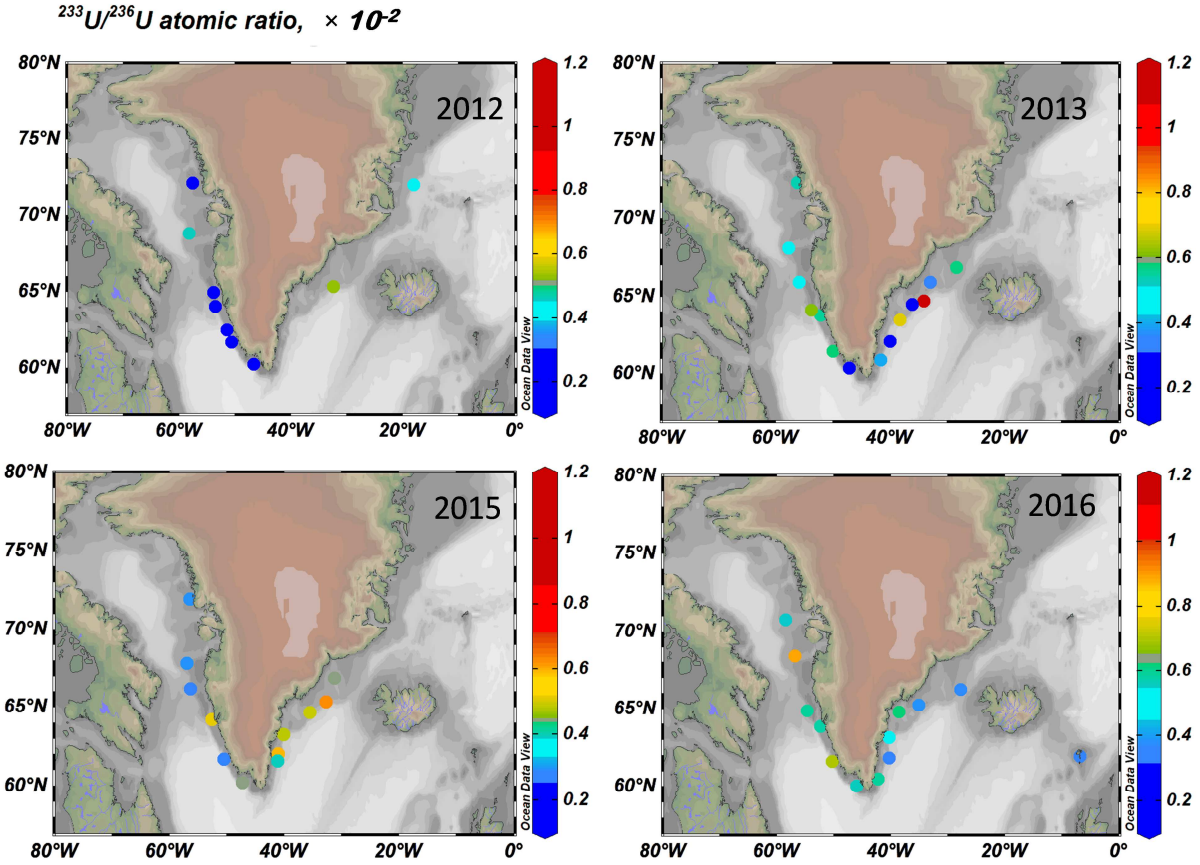

Figure. 4 Box-plots of yearly (a) $^{236}U/^{238}U$ atomic ratio, (b) ^{236}U concentration and (c) $^{233}U/^{236}U$ atomic ratio for samples from Eastern (E) and Western Greenland (W) coast (^{236}U results for sample 2013-0537 and 2013-538 are excluded in the plots). The red cross represents the arithmetic mean value of all the data for a given year, the whiskers extend from minimum (MIN) to maximum (MAX), the green box comprises of first quartile Q1 (top line), median (middle line) and third quartile Q3 (bottom line).

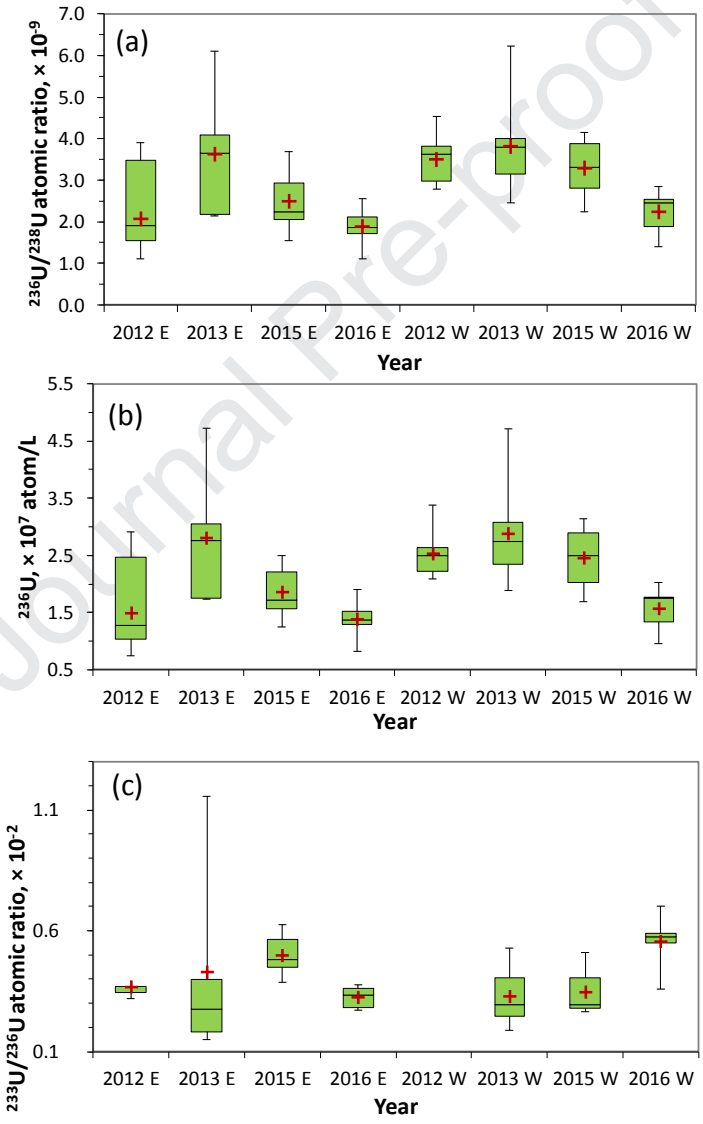

Figure. 5 Ternary mixing diagram of $^{233}U/^{236}U$ and $^{236}U/^{238}U$ atomic ratios for Greenland seawater (2012-2016).

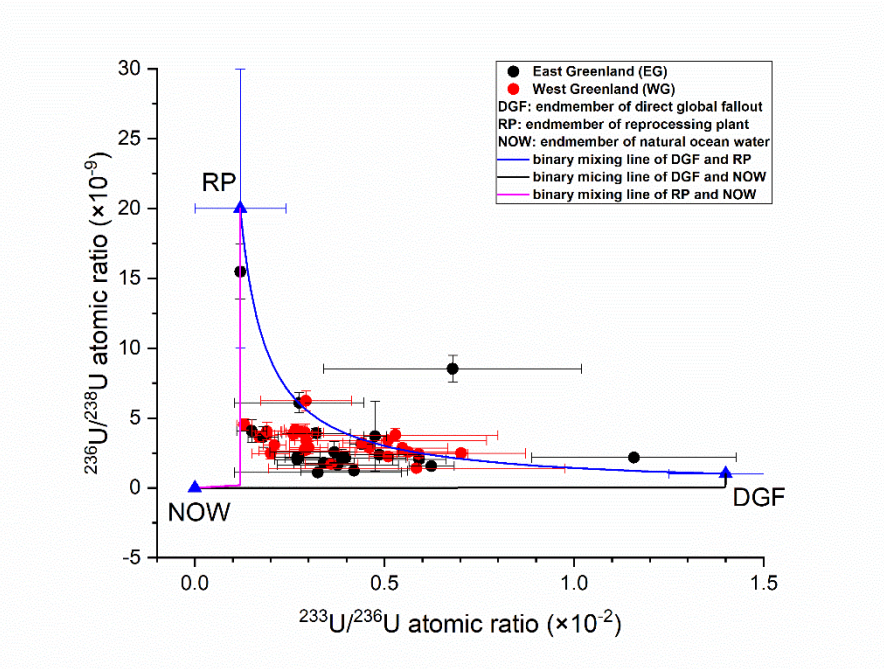

Figure. 6 Variation of calculated concentration of reactor ^{236}U for Greenland seawater (2012-2016) with longitude.

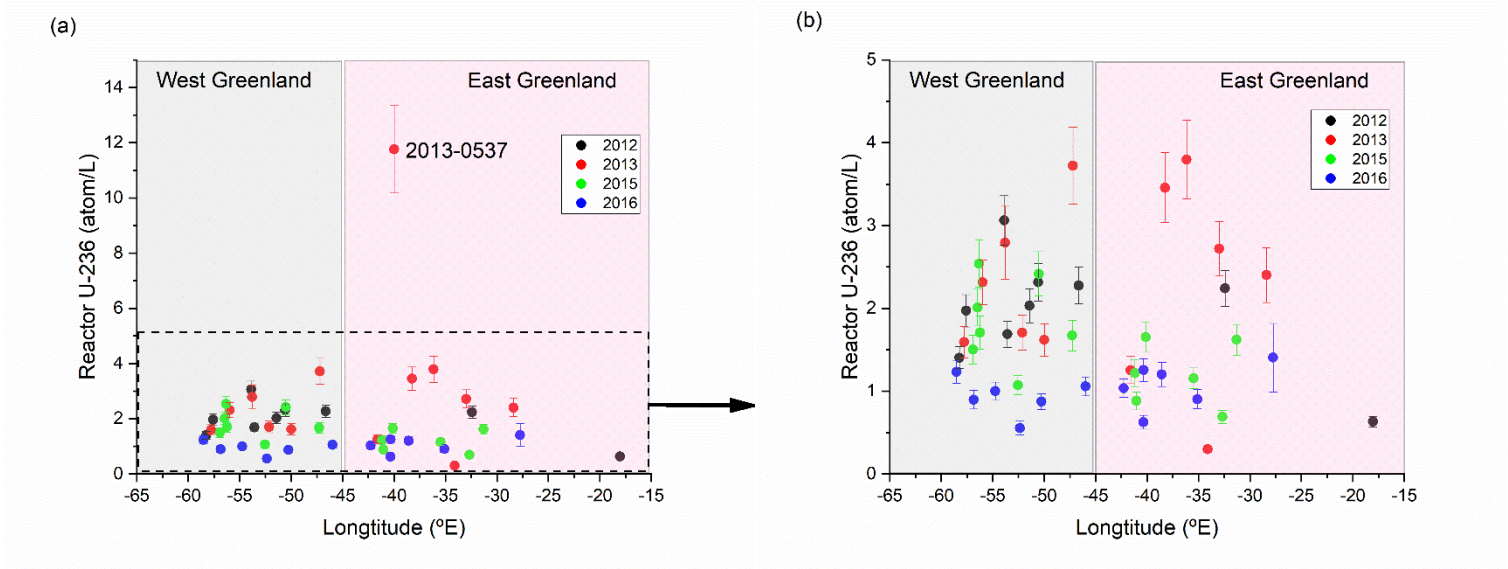

Highlights

- First results of ^{236}U and ^{233}U in the Greenland marine environment.
- ^{236}U concentration in Greenland seawater has a narrow distribution range.
- No significant difference in ^{236}U level between east and west Greenland coast.
- Binary mixing using $^{233}U/^{236}U$ and $^{236}U/^{238}U$ for interpret ^{236}U source term.
- ^{236}U source contribution is calculated based on $^{233}U/^{236}U$ atomic ratios.

Author contribution statement

Jixin Qiao: Conceptualization, Formal analysis, Methodology, Investigation, Resources, Data curation, Writing- Original draft preparation.

Karin Hain: Investigation, Methodology, Data Curation, Resources, Writing- Reviewing and Editing.

Peter Steier: Investigation, Methodology, Data Curation, Resources, Writing- Reviewing and Editing.

Declaration of interests

☒ The authors declare that they have no known competing financial interests or personal relationships that could have appeared to influence the work reported in this paper.

☐The authors declare the following financial interests/personal relationships which may be considered as potential competing interests: